Biochimica et Biophysica Acta 1842 (2014) 2049–2059

Contents lists available at ScienceDirect

Biochimica et Biophysica Acta

journal homepage: www.elsevier.com/locate/bbadis

S100A4 regulates the Src-tyrosine kinase dependent differentiation of Th17 cells in rheumatoid arthritis

Mikael Brisslert [a], Li Bian [a], Mattias N.D. Svensson [a], Rita F. Santos [b], Ing-Marie Jonsson [a], Igor Barsukov [d], Malin Erlandsson [a], Karin Andersson [a], Alexandre M. Carmo [b,c], Maria I. Bokarewa [a,*]

[a] Department of Rheumatology and Inflammation Research, The Sahlgren's Academy at University of Gothenburg, Sweden
[b] IBMC — Instituto de Biologia Molecular e Celular, University of Porto, Portugal
[c] ICBAS — Instituto de Ciencias Biomedicas Abel Salazar, University of Porto, Portugal
[d] Department of Structural and Chemical Biology, Institute of Integrative Biology, University of Liverpool, United Kingdom

ARTICLE INFO

Article history:
Received 14 February 2014
Received in revised form 1 July 2014
Accepted 2 July 2014
Available online 15 July 2014

Keywords:
S100A4
Th17 cell
TCR
Src-tyrosine kinase
Arthritis
CD5

ABSTRACT

Objectives: To evaluate the role of S100A4, a calcium-binding regulator of nonmuscle myosin assembly, for T-cell responses in rheumatoid arthritis. *Methods*: Arthritis was induced in the methylated bovine serum albumin (mBSA)-immunized mice lacking the entire S100A4 protein (S100A4KO) and in wild-type counterparts treated with short hairpin ribonucleic acid (shRNA)-lentiviral constructs targeting S100A4 (S100A4-shRNA). The severity of arthritis was evaluated morphologically. T-cell subsets were characterized by the expression of master transcription factors, and functionally by proliferation activity and cytokine production. The activity of the Scr-kinases Fyn and Lck was assessed by the autophosphorylation of C-terminal thyrosine and by the phosphorylation of the CD5 cytodomain. The interaction between S100A4 and the CD5 cytodomain was analysed by nuclear magnetic resonance spectrophotometry. *Results*: S100A4-deficient mice (S100A4KO and S100A4-shRNA) had significantly alleviated morphological signs of arthritis and joint damage. Leukocyte infiltrates in the arthritic joints of S100A4-deficient mice accumulated Foxp3$^+$ Treg cells, while the number of RORγt$^+$ and (pTyr705)STAT3$^+$ cells was reduced. S100A4-deficient mice had a limited formation of Th17-cells with low retinoic acid orphan receptor gamma t (RORγt) mRNA and IL17 production in T-cell cultures. S100A4-deficient mice had a low expression and activity of T-cell receptor (TCR) inhibitor CD5 and low (pTyr705)STAT3 (signal transducer and activator of transcription 3), which led to increased (pTyr352)ZAP-70 (theta-chain associated protein kinase of 70 kDa), lymphocyte proliferation and production of IL2. *In vitro* experiments showed that S100A4 directly binds Lck and Fyn and reciprocally regulates their kinase activity towards the CD5 cytodomain. Spectrometry demonstrates an interaction between the CD5 cytodomain and EF2-binding sites of S100A4. *Conclusion*: The present study demonstrates that S100A4 plays an important part in the pathogenesis of arthritis. It controls CD5-dependent differentiation of Th17 cells by regulating the activity of the Src-family kinases Lck and Fyn.

1. Introduction

Rheumatoid arthritis (RA) is a progressive debilitating autoimmune disease, which affects 0.5–1% of the total world population [1–3]. Development of RA is characterized by the inflammatory cell infiltration and severe damage of the affected joints. Mature T-cells are the dominating cellular component of the inflamed and hyperplastic synovia in RA [4]. Intervention in T-cell receptor (TCR) activation by minimizing co-stimulation is proved as an efficient treatment strategy in RA [5] and confirms the central role of T-cells in the pathogenesis of this disease.

Appropriate T-cell responses and the strength of the TCR interaction are linked to cytoskeleton reorganisation, where filamentous actin and nonmuscle myosin II (NMMII) play the major part [6,7]. The activation of TCR recruits effector molecules, where the Src-tyrosine kinases Lck and Fyn play a central part in transmitting a TCR/CD3 signal by phosphorylating ITAMs and activating the tyrosine kinase ZAP-70 [8], and recruits cytoskeletal remodelling factors of the Rho GTPase family to the inner leaflet of the cell membrane. The Rho GTPases are coupled to actin and NMMII, and define the duration of TCR activation [6,7]. The diversion of the NMMII function abolishes the formation of TCR clusters at the outer edge of the T-cell [9] and reduces the activity of Src-tyrosine

Abbreviations: mBSA, methylated bovine serum albumin; WT, wild-type; KO, knock-out; IFNγ, interferon-gamma; IL, interleukin; RORγt, retinoic acid orphan receptor gamma t; RA, rheumatoid arthritis; TNF, tissue necrosis factor; TCR, T-cell receptor; Th, helper T cell; STAT3, signal transducer and activator of transcription 3; ZAP-70, theta-chain associated protein kinase of 70 kDa; RhoA, Ras homolog gene family, member A; IRF4, interferon regulatory factor 4; Fak, focal adhesion kinase; ROCK2, Rho-associated protein kinase 2; MHCII, major histocompatibility complex class II

* Corresponding author at: Department of Rheumatology and Inflammation Research, University of Gothenburg, Guldhedsgatan 10A, Box 480, 405 30 Gothenburg, Sweden. Tel.: +46 31 3424021; fax: +46 31 823925.
E-mail address: maria.bokarewa@rheuma.gu.se (M.I. Bokarewa).

http://dx.doi.org/10.1016/j.bbadis.2014.07.003
0925-4439/

kinases in T-cells [10]. In the present study, we evaluated the role of S100A4, a regulator of NMMII assembly and an inhibitor of its ATPase activity, in TCR-dependent immune responses and differentiation of T helper subsets.

S100A4 is a small Ca-binding protein known for its metastasis-promoting properties. It is required for normal cell-to-cell interactions and cell motility. In normal cells and tissues, including fibroblasts, macrophages, lymphocytes, and bone marrow-derived haematopoietic progenitors, the increased expression of S100A4 is observed during cell differentiation, and in angiogenesis and organogenesis [11,12]. Over-expression of S100A4 is seen in many types of tumour cells and leads to epithelial–mesenchymal transition and connects S100A4 to its metastasis promoting properties.

The function of S100A4 is best characterized in interaction with cytoskeletal proteins NMMII, F-actin, and tropomyosin. The binding of S100A4 to these proteins occurs in a Ca^{2+}-dependent manner and inhibits the actin-regulated ATPase activity of myosin II [13,14]. The disassembly of myosin filaments occurring as a result of S100A4 binding is viewed as the major impact of S100A4 in cytoskeletal rearrangements, cell polarization, shape changes, and motility [13,15,16]. Recent reports suggest that S100A4 forms a complex with rhotekin, an adaptor molecule to the cytoskeletal remodelling factor RhoA, and is predicted to regulate RhoGTPase-dependent membrane ruffling [17]. S100A4 binds tumour suppressor p53 in the *in vitro* purified system [18] and in cells [19–22]. Binding of S100A4 to p53 occurs in the cell nucleus and initiates its degradation.

The binding of S100A4 to calcium drives conformational changes and permits S100A4 to regulate the activity of its multiple intracellular protein partners placing S100A4 at the crossroad of several intracellular transduction mechanisms. Intracellular S100A4 controls signal transduction through FcγRIIIA by inhibiting the activation of the tyrosine kinase Syk [23]. S100A4 is described as an essential partner of the JAK/STAT signal transduction activating receptors to IL7 in chondrocytes [24] and IL10 in the cells of neuroglia [25]. S100A4 is required for the IL1 receptor dependent activation of an ERK–p38–JNK signalling pathway [26] and for mediating estrogen effects to bone progenitors [27]. S100A4 binds transcription factor Smad3 and enhances TGFγ-mediated effects by promoting cancer invasiveness [28] and autoimmune inflammation [29].

In RA, S100A4 is abundantly expressed in synovial fibroblasts, macrophages and vascular endothelial cells of the inflamed joints and may be measured in synovial fluid and in blood [30,31]. The clinical consequences of the high levels of S100A4 in RA patients are associated with resistant joint inflammation and high skeletal damage [32,33]. The current view on the function of S100A4 is consistent with its extracellular regulation of local inflammation by stimulating the production of matrix metalloproteinases in synovial fibroblasts and in chondrocytes [26,31].

In the present study we show that S100A4 is essential for T-cell maturation and function controlling TCR-dependent immune responses. These results are consistent in two independent *in vivo* models of S100A4-deficiency, the knock-out mice obtained by the germ-line inactivation of the S100A4 gene, and the acute inhibition of the S100A4 gene transcription by specific shRNA-producing constructs. S100A4 directly binds the Src-kinases Lck and Fyn and reciprocally regulates their kinase activity. S100A4-deficiency results in a reduced activity of STAT3 suppressing transcription of RORγt and lineage differentiation of Th17 cells. The immunological events controlled by S100A4 are functionally important for the pathogenesis of arthritis, since the deficiency in S100A4 alleviates experimental arthritis.

2. Materials and methods

2.1. Mice

S100A4 knockout mice (S100A4KO) were generated on an A/Sn background by a germ-line inactivation of the *S100A4* gene as described in [34,35]. The breeding pairs of S100A4KO and congenic WT (A/Sn) mice were kindly provided by Dr. Mariam Grigorian, Institute of Cancer Biology, Copenhagen. Mice were bred at the animal facility of the Department of Rheumatology and Inflammation Research, University of Gothenburg. The mice were housed 8–10 animals/cage with a 12 h light and dark cycle, and fed with standard laboratory chow and water *ad libitum*. All animal experiments are approved by the Animal Experimental Board of the Gothenburg University (permits 2009-88, 319-2011 and 125-2012).

2.2. Arthritis model

Arthritis was induced by the intra-articular injection of 30 μg methylated bovine serum albumin (mBSA, Sigma Aldrich) in the left knee of preimmunised animals as described in [36]. Mice were immunized subcutaneously with mBSA emulsified with the complete Freund's adjuvant (Sigma Aldrich) on day 0 and day 7. The left knee joint was injected with mBSA on day 21 and the morphological evaluation was done on day 28. In total, 33 S100A4KO-mice and 33 WT mice were used in 3 independent experiments. Each experiment contained S100A4KO and WT male littermates, 6–10 mice/group.

2.3. Down-regulation of S100A4 in vivo

Fifteen WT (A/Sn) mice were treated with the bioconstructs containing sequences coding for the S100A4 gene targeting shRNA and a lentiviral vector (Sigma-Aldrich, St. Louis, MO, USA); an additional 7 WT mice received a non-targeting bioconstruct. Mice were treated with 1×10^7 transduction particles/mouse and the successful inhibition of the S100A4 gene transcription was proved by Western blot as described in [37].

2.4. Adoptive transfer

$CD4^+$ T cells were purified on the magnetic beads using the mouse $CD4^+$ T cell isolation kit (StemCell Technology). The purity and viability of the isolated $CD4^+$ T cells were 89% and 98%, respectively. The isolated $CD4^+$ T cells were injected i.v. into the recipient mice (S100A4KO, $n = 7$; and WT mice, $n = 8$). Each mouse obtained 2×10^6 of the CD^+ T cells. S100A4KO mice ($n = 6$) were used as controls. At the same day of $CD4^+$ T cell transfer, mice were subjected to the arthritis model as above and sacrificed on day 28.

2.5. Clinical and histological evaluation of arthritis

The histological evaluation of the mBSA-injected knee joints was done on the paraffin-embedded and haematoxylin and eosin stained sections. The sections were coded and evaluated for signs of inflammation and cartilage/bone destruction. Arthritis was evaluated on an arbitrary scale from 0 to 3 [36]. The representative histological figures of the arthritis scale are shown in Fig. 1A.

2.6. Immunohistochemisty staining

The paraffin-embedded sections of knee joints were subjected to antigen retrieval as described in [38], and blocked with 0.3% H_2O_2, serum solution (Vector laboratories) and Fc-block (BD Pharmingen™). After incubation with rabbit anti-mouse pSTAT3 (Tyr705, AbCam), IL17 (AbCam), RORγt (eBioscience), and Foxp3 (eBioscience) antibodies or rabbit gammaglobulins (Jackson) as a negative control, the specimens were incubated with ImmPRESS anti-rabbit Ig polymer detection reagent and stained using ImmPACT™ AEC (Vector laboratories), and Mayer's haematoxylin (Histolab).

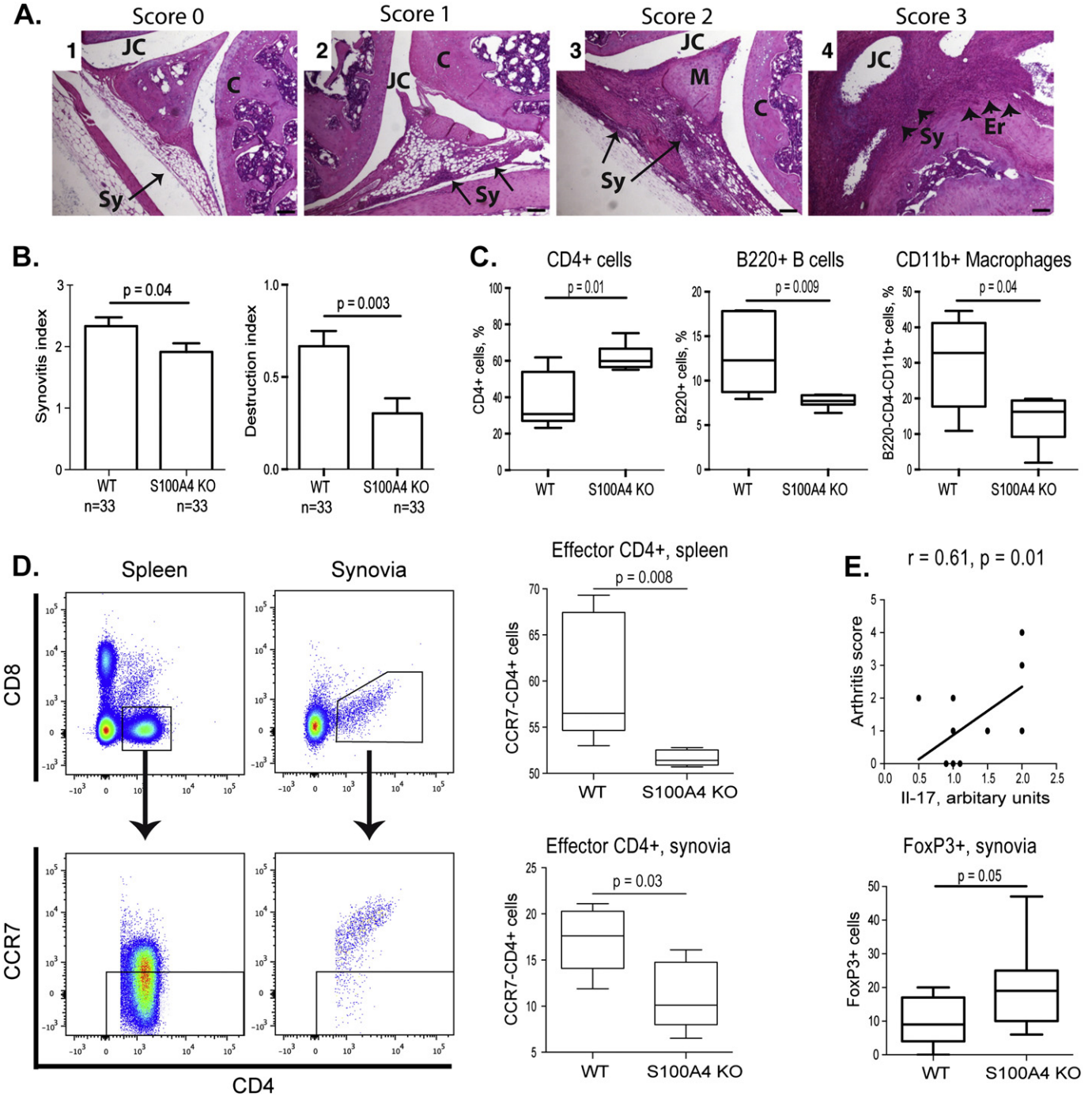

Fig. 1. S100A4 deficiency alleviates mBSA-induced arthritis by changing the composition of Th-cells in the synovial tissue. A. Severity of arthritis was scored in the haematoxilin–eosin stained section of knee joints using the arbitrary scoring system, where (0) presents normal synovia (Sy). The joint cavity (JC) and cartilage (C) are preserved, no inflammatory cells are seen. (1) Small clusters of inflammatory cells are found in synovia (arrows). The joint cavity and the cartilage are preserved. (2) Substantial inflammatory cell infiltrates are spread in the synovial tissue. (3) Inflammatory cells fill the whole joint cavity. Loss of cartilage integrity is indicated as erosions (Er). (M) = meniscus. B. The synovitis index and destruction index were calculated for S100A4-deficient (S100A4KO, n = 33) and wild-type mice (WT, n = 33). C. Cell composition of the inflamed synovial tissue was assessed by flow cytometry in S100A4KO mice (n = 8) and in WT mice (n = 9). D. The effector $CD4^+CCR7^-$ cells were analysed in synovial tissue and in the spleen of the mBSA-immunization mice. Dot plots show the gating strategy used for the analysis. S100A4KO mice had smaller populations of the effector $CD4^+CCR7^-$ cells in the knee synovia and in the spleen. E. The expression of IL17 in the inflamed synovial tissue correlated with the arthritis index in the joints of S100A4KO and WT mice. S100A4KO mice had a higher number of $FoxP3^+$ cells in the knee synovia compared to WT mice.

2.7. Western blotting

Total protein was prepared from spleen tissue in the presence of protease and phosphatase inhibitors (Complete Mini and Phospho Stop; Roche Diagnostics GmbH, Mannheim, Germany). Protein concentrations were measured using the bicinchoninic protein assay kit (Pierce, Thermo Scientific, Rockford, Illinois). Proteins were separated on SDS-PAGE 4%–12% Bis–Tris gels (NuPAGE; Life technologies Ltd., Paisley, United Kingdom) and transferred to polyvinyl difluoride membranes (Life Technologies). Membranes were blocked with 5% BSA and incubated with antibodies against S100A4 (Dako; A5112), pSTAT3 (Abcam; ab76315), or actin (Sigma; A2066) at 4 °C overnight.

Detection was performed with peroxidase-conjugated anti-rabbit secondary antibody (NA934VS; GE Healthcare, Uppsala, Sweden) and ECL substrate (Amersham Biosciences, Uppsala, Sweden). Chemiluminescent signals were quantified by the Chemidoc gel documentation system using Quantity-One software (Bio-Rad Laboratories, Hercules, California).

2.8. Stimulation of spleen and synovial cell cultures

Cells cultures of spleen and synovial tissue were prepared as previously described [36] and resuspended to the concentration 2×10^6 cells/ml in Iscove's complete medium (10% fetal calf serum, 4 mM L-glutamine, 50 μM β_2-mercaptoethanol, and 20 μg/ml gentamicin). Cultures were stimulated with anti-CD3 antibodies (1 μg/ml, R&D Systems), or LPS (10 μg/ml, Sigma-Aldrich). The supernatants were collected for cytokine analysis after 48 and 72 h. For the intracellular phosphorylation analysis cells were rested for 24 h and stimulated with anti-CD3 (2 μg/ml). Stimulation was stopped after 2 min, 5 min, and 10 min by the addition of PFA (1.5%/v).

2.9. Splenocyte proliferation

The cells were labelled with a cell trace Violet dye binding to intracellular amines (InVitrogene) prior to stimulation. The reduction in the dye indicates the lymphocyte proliferation rate. The alternative read-out system included the incorporation of ^{3}H-thymidine (Perkin Elmer, Boston, MA, USA) added to the cell cultures 12 h before cell harvest, as previously described [38].

2.10. Flow cytometry

Cells were incubated with F_c-block (BD Pharmingen) and stained with primary antibodies against CD4 (GK1.5), CCR7 (4B12), CD5 (53–7.3), B220 (RA3-6B2), CD11b (M1/70), CD11c (HL3), F4/80 (BM8) (all from BD Biosciences) and CD62L (MEL-14) (Biolegend). For the intracellular phosphorylation analysis cells were stained with rabbit anti-CD5 (pTyr453, Antibodies-online, Atlanta, GA, USA), or ZAP-70 (pTyr319/Syk pTyr352, Thermo Scientific, Rockford, IL, USA), or Fyn (pTyr530, Santa Cruz Biotechnology, Santa Cruz, CA, USA) and visualised by Alexafluor647-conjugated goat-anti-rabbit antibody (Molecular Probes, LifeTechnologies, Stockholm, Sweden). For intracellular RORγt staining clone B2D, and clone eBRG1 as IgG1 isotype control (eBioscience, San Diego, CA, USA) were used.

Cells were collected 5×10^5 events/spleen sample, and 1×10^4 events/synovial sample using a FACSCantoII (BD Bioscience) equipped with FACSDiva software. The analysis was performed using FlowJo software (version 10.0.6, Tree Star, Inc., Ashland, OR). The fluorochrome compensation was done on CompBeads (BD Bioscience).

2.11. Cytokine analyses

Cytokines were measured in supernatants of splenocyte cultures diluted 1:2 by flow cytometry using a CBA kit (BD Bioscience). The lower detection limits for IL2, IL4, IL6, IFNγ, TNFα, IL17A, and IL10 were 0.1 pg/ml, 0.03 pg/ml, 1.4 pg/ml, 0.5 pg/ml, 0.9 pg/ml, 0.8 pg/ml and 16.8 pg/ml, respectively.

2.12. Gene expression analysis

Total RNA was extracted from splenocytes using an RNeasy Mini Kit (Qiagen, Valencia, CA). The quality of RNA samples was evaluated with Experion (Bio-Rad Laboratories Inc., USA). Real-time amplification was performed with RT^2 SYBR® Green qPCR Mastermix (Qiagen) using a ViiA™ 7 Real-Time PCR System (Applied Biosystems) as previously described [37]. The expression of the following genes was measured (S100A4 (Mts-1), Foxp3, Gata3, Tbx21, RORγt, IRF4, IL21, Ki67, CD5, Bcl6 and Blimp1) and normalised to the reference genes *Gapdh* and *Ppia*. The sequences of primers and probes used in the qPCR are available from Applied Biosystems. The results were expressed as the fold change (relative quantification (RQ)) compared with the expression levels in the WT control cells with the ddCt-method.

2.13. In vitro kinase assays and precipitation of phosphorylated CD5 peptide

Kinase assays were performed as previously described [39]. When indicated, S100A4 or BSA as control was included in the kinase reaction. Antibodies used for immunoprecipitation and immunoblotting were polyclonal anti-Fyn (BL90) and anti-Lck (DA3), kind gifts from M. G. Tomlinson (University of Birmingham), and anti-Csk (Santa Cruz Biotechnology). Densitometric quantitation of the autoradiographs was done on a GS-800 densitometer (Bio-Rad) using the Quantity One software (Bio-Rad). Densitometric values are expressed in arbitrary units calculated from background non-saturated signals.

A biotinylated peptide containing the rat CD5 ITAM-like sequence (Biot-AASHVDNEYSQPPRNSRLSAYPALE-OH, purchased from New England Peptide) was also included as a Fyn or Lck substrate in the reaction mix at a final concentration of 0.5 μg/μl. For the precipitation of the biotin-labelled CD5 peptide, the beads containing the immune complexes were boiled for 5 min in 2% SDS and diluted 8-fold with lysis buffer. After centrifugation, supernatants were recovered and pre-cleared for 30 min with 100 μl protein A Sepharose beads. The CD5-peptide was recovered using neutravidin beads (Thermo Scientific) and the incorporated [γ-^{32}P]-ATP was measured in a Beckman liquid scintillation counter.

2.14. Nuclear magnetic resonance spectroscopy

^{15}N-labelled S100A4 was expressed and purified as described in [15]. Synthetic peptide NEYSQPPRNSHLSAYPALEGALHRSSTQPDNSSDSDYDL corresponding to residues 450–488 aa of CD5 was purchased from ChinaPeptides (Shanghai); the peptide was purified by HPLC to >95%, and sequence was confirmed by mass spectrometry. NMR experiments were conducted in 20 MES, 40 NaCl, 5 $CaCl_2$, pH 6.1 buffer at 40 °C. 100 μM S100A4 was titrated with a 5 mM CD5 peptide solution. The concentrations of S100A4 and CD5 peptide were determined from the UV absorbance at 280 nm. ^{1}H,^{15}N-HSQC spectra were recorded on a Bruker AVANCE-II 600 MHz spectrometer equipped with CryoProbe. Proton chemical shifts were referenced to external DSS. Spectra were processed with TopSpin (Bruker) and analysed using ANALYSIS [40].

2.15. Statistical analysis

Values are reported as median and inter-quartile range [IQR]. Comparisons between groups were performed using the Mann–Whitney *U* test. A p value < 0.05 was considered significant.

3. Results

3.1. Arthritis and bone destruction are decreased in S100A4KO mice

Arthritis was induced in the mBSA-immunized S100A4KO and WT mice by an injection of mBSA into the left knee joint. Histological evaluation of the injected joints was performed 7 days later by a semi-quantitative scoring (Fig. 1A). The arthritis scoring included the mononuclear cell infiltration (synovitis), synovial growth forming above the cartilage (pannus) and the loss of bone integrity (erosion). The histological analysis revealed that S100A4KO mice had a low synovitis index ($p = 0.04$), and a low destruction index ($p = 0.003$) compared with WT mice (Fig. 1B).

Flow cytometry of the inflamed synovia of S100A4KO mice revealed a higher proportion of CD4$^+$ T cells and a lower proportion of

macrophages ($B220^{-}CD4^{-}CD11b^{+}$) and B-cells ($B220^{+}$) compared to WT mice (Fig. 1C). S100A4KO mice had a reduced number of effector $CD4^{+}$ T-cells in the inflamed synovial tissue ($CCR7^{-}$, $p = 0.008$) and in the spleens ($CCR7^{-}$, $p = 0.008$) (Fig. 1D). The synovial infiltrates in S100A4KO mice were enriched with $Foxp3^{+}$ cells compared to WT (Fig. 1E). The number of $ROR\gamma t^{+}$ cells was low in the synovia of S100A4KO mice, while IL17 staining was similar between S100A4KO and WT mice and correlated to the arthritis severity.

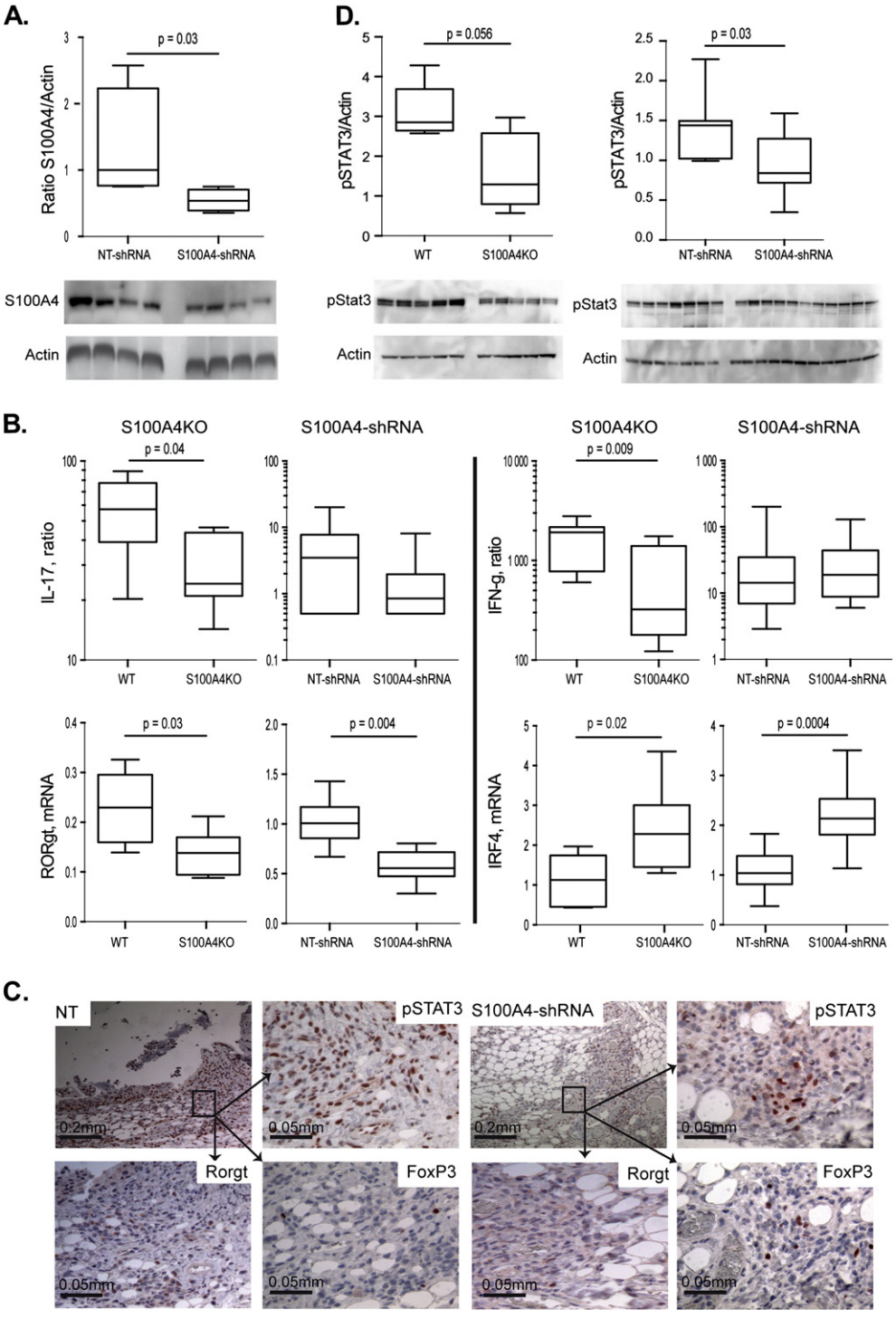

Fig. 2. S100A4 deficiency limits the formation of Th17-cells. A. Inhibition of S100A4 was achieved by an intra-peritoneal injection (1×10^{7} transduction particles/mouse) of a specific lentiviral construct targeting the gene of S100A4 (S100A4-shRNA) in WT mice. Control mice were injected with non-targeting (NT)-RNA. Protein levels of S100A4 were assessed in shRNA-treated and NT mice by Western blot and quantified in relation to actin. Each line represents an individual mouse. B. Levels of IL17 and IFNγ were measured in supernatants of spleen cell cultures stimulated with aCD3 (3 μg/ml) by a CBA-kit. Levels of transcription factors RORγt and IRF4 mRNA in the spleen were assessed by RT-PCR. The mRNA levels in S100A4KO and S100A4-shRNA treated mice are quantified as the fold difference (RQ) compared with WT and NT-RNA cells with the ddCt-method. C. Synovial tissue of WT mice treated with S100A4-shRNA and NT-shRNA was stained for the presence of cells expressing active STAT3 (pTyr705), RORγt, and FoxP3. The area of higher magnification is gated. The positive cells are stained orange, and cell nuclei are stained with haematoxylin. D. The levels of active (pTyr705)STAT3 are quantified as a ratio to actin in spleens of S100A4KO and S100A4-shRNA treated mice and compared with control WT mice and NT-shRNA treated mice. Each line in the Western blot represents an individual mouse. Statistical evaluation was performed using the Mann–Whitney analysis and p-values equal or below 0.05 were considered significant.

3.2. S100A4 deficiency alters maturation of the effector Th17 cells

To prove the role of S100A4 in the changes observed in the T-cell phenotype, we induced an acute inhibition of the S100A4 gene by a specific shRNA-lentiviral construct (S100A4-shRNA). The intra-peritoneal injection of WT mice with the S100A4-shRNA resulted in a significant reduction of S100A4 protein in spleen (Fig. 2A).

The analysis of T helper (Th)-cells in spleen cultures of S100A4-deficient (S100A4-shRNA treated and S100A4KO) mice revealed a low production of IL17A following aCD3-stimulation, while the levels of IFNg was low in S100A4KO mice (Fig. 2B). Expression of the Th17 specific transcription factor RORγt mRNA was also reduced in S100A4KO and in S100A4-shRNA treated mice (Fig. 2B), while the Th1 transcription factor T-bet was similar to WT and NT-shRNA treated controls (not shown). The leukocyte infiltrates of the arthritic synovia of S100A4-shRNA treated mice was enriched with Foxp3$^+$ cells and had a lower number of RORγt$^+$ cells (Fig. 2C). This confirmed that the impaired formation of Th17 effector T-cells was dependent on S100A4.

3.3. S100A4-deficient mice display an impaired transcriptional control over lineage differentiation of Th17 cells

The initial lineage commitment of Th17 cells is controlled by transcription factors IRF4 and STAT3 [41]. Assessment of these transcriptional factors in spleens of S100A4-deficient mice revealed a significant increase of IRF4 mRNA both in S100A4KO mice and in S100A4-shRNA-treated mice (Fig. 2B). Splenocytes of S100A4-shRNA-treated mice had high Blimp-1 mRNA ($p = 0.02$). The active STAT3 was measured by the phosphorylated (p)Tyr705-STAT3 in spleen cells. Western blot analysis showed that S100A4KO and S100A4-shRNA-treated mice had reduced levels of pTyr705-STAT3 ($p = 0.056$ and $p = 0.03$, respectively, Fig. 2D). Additionally, the low number of pSTAT3$^+$ cells was present in the inflamed joints of S100A4KO and S100A4-shRNA-treated mice (Fig. 2C). These findings suggest that the low activity of STAT3 may be responsible for the low transcription of RORγt in S100A4-deficient mice.

3.4. S100A4 deficiency increases lymphocyte proliferative response

STAT3-deficient T cells have a high proliferation and high production of IL2 [44]. Consistent with the low pTyr705-STAT, S100A4KO mice had an increased lymphocyte proliferation response to stimulation with aCD3 ($p = 0.029$, Fig. 3A), LPS (B-cell ratio, 4.58 [3.8–5.1] *vs.* 1.9 [1.7–2.3], $p = 0.028$) and mBSA ($p = 0.0003$). S100A4-shRNA treated mice had a similar increase in the proliferation response (Fig. 3B). To prove the role of S100A4 for T cell function, we performed a transfer of CD4$^+$ T cells of WT mice to S100A4KO recipients. The proliferative response assessed in S100A4KO recipients 28 days after the transfer showed a reduction compared to non-transferred S100A4KO mice (Fig. 3A).

The increased proliferative ability in S100A4-deficient mice was combined with higher levels of Ki-67 mRNA (Fig. 3C) and IL2 protein levels (Fig. 3D). The adoptive transfer of WT CD4$^+$ T cells into S100A4KO mice increased the population of RORγt$^+$CD4$^+$ T cells in the recipient mice (Fig. 3E).

3.5. S100A4-deficiency reduces surface expression and activity of CD5

Modulation of TCR signalling is attributed to major functional effects of CD5 [43]. S100A4-deficient mice had a smaller population of CD5$^+$CD4$^+$ T cells compared to WT controls (Fig. 4A). The adoptive

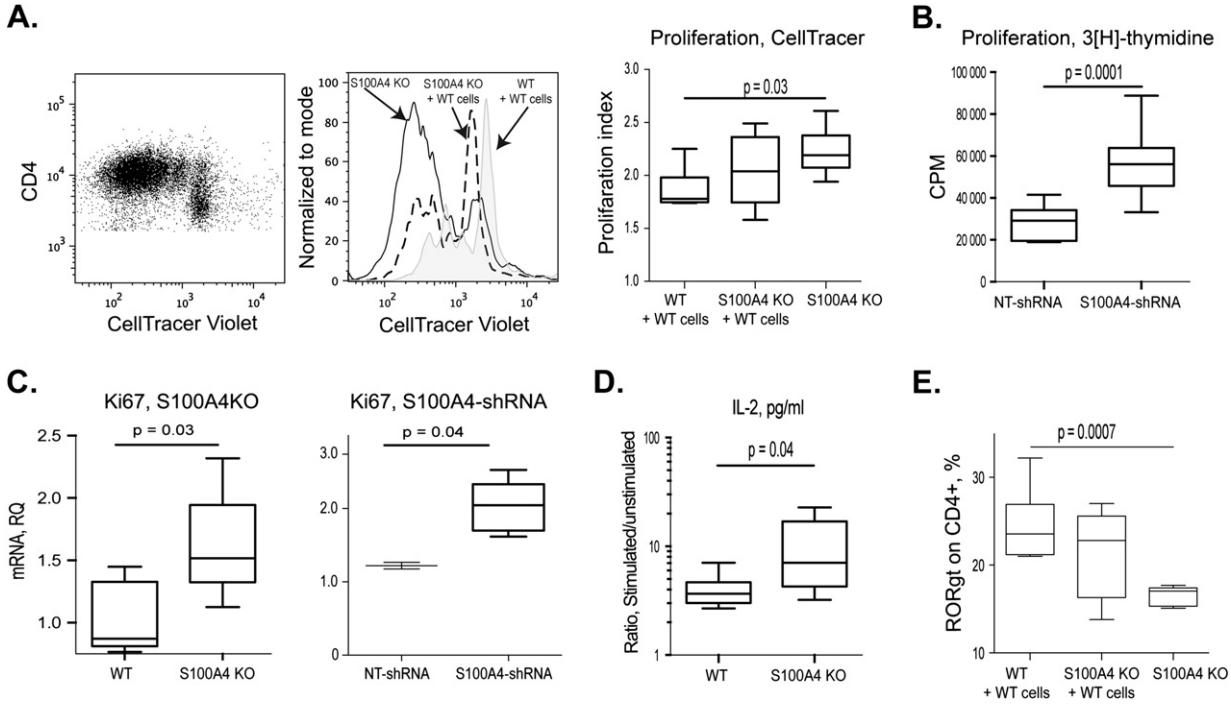

Fig. 3. S100A4 deficiency increases lymphocyte proliferation. A. Lymfocyte proliferation was assessed in aCD3 (3 μg/ml) stimulated spleen cultures of S100A4KO mice (n = 6), S100A4KO recipients of CD4$^+$ WT cells (2×10^9 cells/mouse, n = 7), or WT recipients of CD4$^+$ WT cells (n = 8) using the membrane CellTracer™ violet staining. A representative dot plot shows the distribution of the cell tracer in proliferating CD4$^+$ cells. The histogram shows proliferating T cells of S100A4KO mice (black solid line), S100A4KO mouse recipients of WT cells (black dashed line), and WT mouse recipients of WT cells (grey filled) after 72 h of aCD3 stimulation. Cells are gated on CD4$^+$ cells. The box plot shows the proliferative response within each group. B. The proliferative response was assessed in S100A4-shRNA and NT-shRNA treated mice by ^{3}[H]-thymidine incorporation following 72 h of aCD3 stimulation. C. Ki67 mRNA levels were measured in aCD3-stimulated spleen cells of S100A4-shRNA or NT-shRNA treated mice by RT-PCR. The results are expressed as the fold difference (RQ) compared with WT control cells with the ddCt-method. D. IL2 levels were measured in the supernatants of aCD3-stimulated spleen cultures of S100A4KO and WT mice using a CBA-kit. The results are as the ratio of IL2 levels in the stimulated/unstimulated supernatant. E. The population of RORγt$^+$CD4$^+$ T-cells was quantified in the spleen of mBSA-immunized S100A4KO mice, S100A4KO mouse recipients of CD4$^+$WT cells, and WT mouse recipients of CD4$^+$WT cells using flow cytometry. Statistical evaluation was performed using the Mann–Whitney analysis and p-values equal or below 0.05 were considered significant.

transfer of WT CD4$^+$ T cells to S100A4KO recipients showed an increase in CD5$^+$ T cell population of the recipients (Fig. 4B). S100A4KO mice displayed low CD5 mRNA ($p = 0.05$), which suggested that the transcription and cell surface expression of CD5 is dependent to S100A4. The S100A4-deficient spleen cultures had low levels of active pTyr453-CD5 (Fig. 4C). Since functional CD5 has been reported as essential for the activation of STAT3 [42], these findings provide a link to the low levels of pSTAT3 in S100A4-deficient mice.

Consistent with the increased proliferation, S100A4-deficient T-cells had increased levels of pTyr352 ZAP-70 compared with WT (Fig. 4D). Importantly, the activity of ZAP-70 was lower in CD5$^+$ T-cells, the population affected in S100A4KO mice. Also, CD5$^+$ cells displayed an

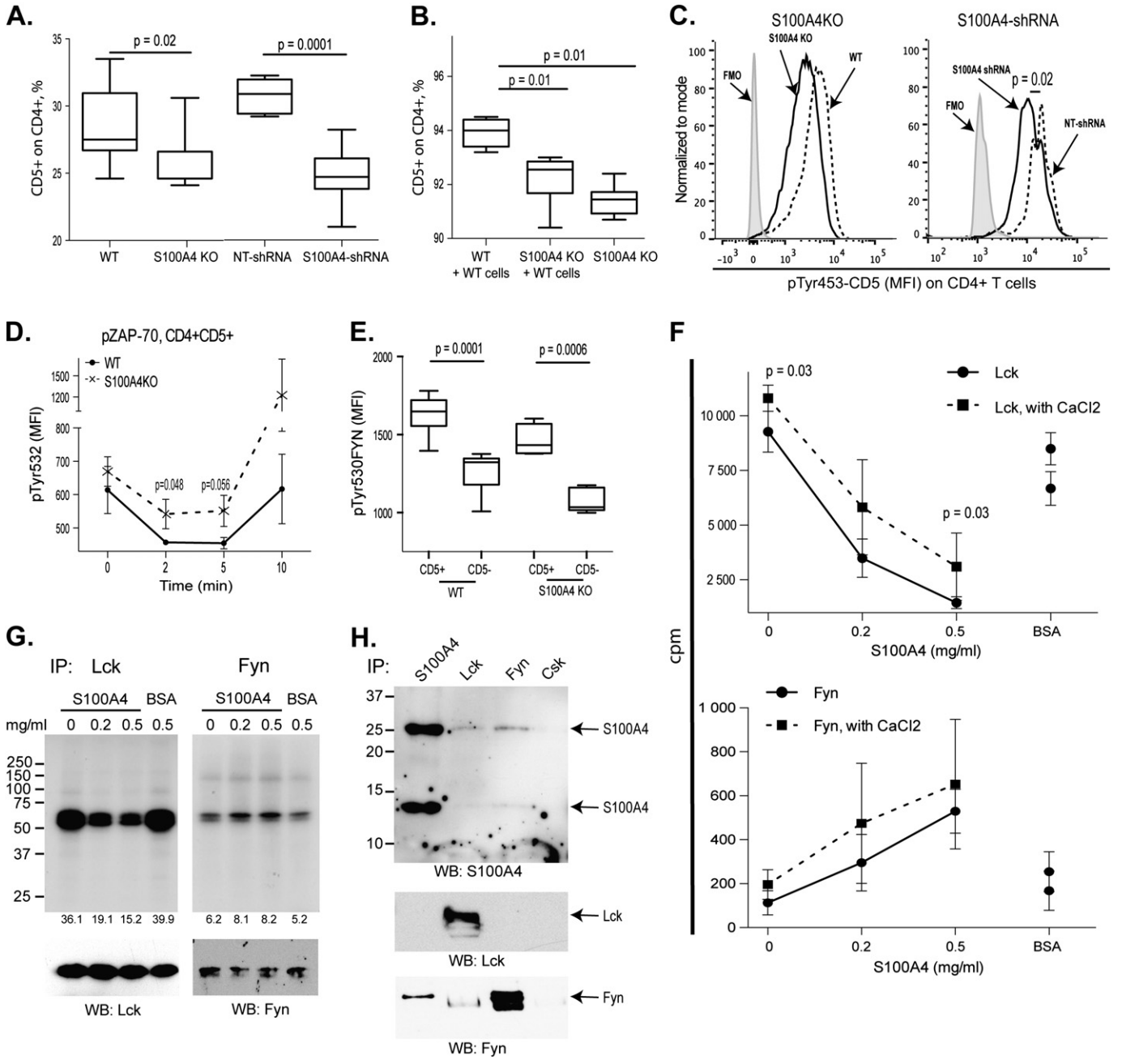

Fig. 4. S100A4 deficiency limits CD5 expression and reduces ZAP-70, Fyn and Lck activity. A. The population of CD5$^+$CD4$^+$ T-cells was assessed in the spleen of S100A4KO and S100A4-shRNA treated mice and their controls by flow cytometry. B. The box plots shows CD5$^+$CD4$^+$ T-cells within splenocytes of S100A4KO mice, S100A4KO mouse recipients of CD4$^+$WT cells, and WT mouse recipients of CD4$^+$WT cells. C. Phosphorylated (p)Tyr453 CD5 on CD4$^+$ T cells was measured by flow cytometry following anti-CD3 (3 μg/ml) stimulation, and presented as the mean fluorescent intensity (MFI). D. Phosphorylated (p)Tyr532 Zap-70 on the CD4$^+$CD5$^+$ T-cells of S100A4 KO and WT mice was measured following aCD3 stimulation by flow cytometry. E. Phosphorylated (p)Tyr530 at C-terminal of Fyn was measured on CD4$^+$CD5$^+$ and CD4$^+$CD5$^-$ T-cells by flow cytometry, and presented as the mean fluorescent intensity (MFI). F. Lck and Fyn were immunoprecipitated from lysates of non-stimulated Jurkat cells. Effect of S100A4 (0–0.2–0.5 mg/ml) on the kinase activity of Lck and Fyn was assessed using a 25 aa-long peptide of CD5 containing tyrosines 453 and 465. Control experiments were performed in the presence of BSA. [γ-^{32}P]-ATP was used as source of the phosphate groups. After the kinase reactions, the peptide was pulled down with neutravidin beads and the radioactivity incorporated into the peptide was measured in a liquid scintillation counter. The experiments performed in Ca-free and $CaCl_2$ enriched buffers gained similar results. The line plots present scintillation counts obtained in 3 independent experiments. Mean ± SEM. G. Changes in the kinase activity with the increasing concentrations of recombinant (r)S100A4 were assessed by autophosphorylation of kinases. The immunoprecipitated Lck and Fyn kinases were subjected to SDS-PAGE and autoradiography. The densitometry values are indicated under each line. H. Lck and Fyn were immunoprecipitated from lysates of Jurkat cells in the presence of rS100A4 (0.1 mg/ml). Antibodies against S100A4 and C-terminal src-kinase (Csk) were used as positive and negative controls, respectively. Immunoblotting of the immunoprecipitates with an anti-S100A4 antibody confirmed that S100A4 was included in the Lck and Fyn immunoprecipitates (upper panel). Fyn was visible in S100A4 immunoprecipitates (lower panel). No Lck could be detected in S100A4 immune complexes (middle panel).

increased activity of pTyr530 Fyn as compared to $CD5^-$ cells in both WT and S100A4KO mice (Fig. 4E).

3.6. S100A4 associates with, and affects the kinase activity of, the Src-tyrosine kinases Lck and Fyn

Lck, and to a lesser extent Fyn, are protein tyrosine kinases which, in parallel with the initiation of a TCR-mediated signal, are involved in the phosphorylation of the inhibitory receptor CD5 [45]. As S100A4 deficiency is translated into the insufficient CD5 and the increase in T-cell proliferation, we asked whether the S100A4 protein could directly obstruct the activity of the Src-tyrosine kinases *in vitro*.

Lck and Fyn were immunoprecipitated from lysates of non-stimulated Jurkat cells (a human T-cell line) and, using [γ-^{32}P]-ATP as a source of the phosphate groups, their kinase activities were assessed in the presence or absence of recombinant S100A4. A synthetic biotinylated peptide corresponding to the C-terminal part of the CD5 cytoplasmic domain and containing two tyrosine residues (Tyr453 and Tyr465) was used as a phosphorylation substrate. After the kinase reaction, the peptide was pulled down with neutravidin beads and the radioactivity incorporated into the peptide was measured in a liquid scintillation counter. Recombinant S100A4 induced a remarkable decrease of peptide phosphorylation mediated by Lck, while it provoked an increase in the phosphorylation regulated by Fyn (Fig. 4F). This effect of S100A4 was calcium-independent, since the addition of $CaCl_2$ had only a marginal effect of the phosphorylation of the peptides. Replacement of S100A4 by control BSA restored completely (for Fyn) or most (for Lck) of the peptide phosphorylation.

To clarify whether these effects were due to changes in the kinases' activities by S100A4 or to a possible block/interference of the phosphorylation sites by S100A4 binding to the peptide, we immunoprecipitated the kinases directly from the reactions and assessed their autophosphorylation capacity. As seen by SDS-PAGE and autoradiography, S100A4 at 0.5 mg/ml provoked a marked decrease of the Lck activity (by 55%), while the activity of Fyn was simultaneously increased by over 30%, as indicated by the densitometry values under each lane (Fig. 4G). Substitution of S100A4 by BSA reverted the activity of the kinases to their original levels.

A direct interaction of S100A4 with both Lck and Fyn was confirmed by co-precipitation of Lck and Fyn with recombinant S100A4 (at 0.1 mg/ml) from lysates of Jurkat cells. Antibodies against S100A4 and Csk (a tyrosine kinase that phosphorylates the inhibitory C-terminal tyrosine residue of Lck and Fyn) were used as positive and negative controls, respectively. Immunoblotting of the immunoprecipitates with an anti-S100A4 antibody confirmed that S100A4 was included in the Lck and Fyn immunoprecipitates (Fig. 4H, upper panel). Reciprocally, Fyn was visible in S100A4 immunoprecipitates (Fig. 4H, lower panel). However, no Lck could be detected in S100A4 immune complexes (Fig. 4H, middle panel). Given that recombinant S100A4 is present in large excess relatively to endogenous proteins in this assay, and that in Jurkat cells Fyn is expressed at much lower levels than Lck, these combined results suggest that the interaction of S100A4 with Fyn is significantly stronger than that of S100A4 with Lck.

3.7. CD5 binds to the EF2 pocket of S100A4

S100A4 changed the activity of Lck and Fyn in the presence of the CD5 peptide. This suggested that S100A4 could bind CD5 directly and therefore block, at least partly, the interaction between S100A4 and the kinases. To ascertain the interaction of S100A4 with the C-terminal region of CD5, NMR binding studies were performed as described in [15]. The addition of a CD5 peptide (aa 450–488) to S100A4 caused a specific chemical shift change in the spectra of Ca^{2+}-bound S100A4 (Fig. 5A), but had no effect on the spectra of apo-S100A4 (not shown). The chemical shifts changed progressively with the increase of the CD5 peptide concentration. No resonance broadening was detected and at 2-fold excess of the CD5 peptide (100 μM S100A4) chemical shift changes did not reached saturation, indicating a relatively weak binding with the dissociation constant $K_D \geq 100$ μM. The significant chemical shift change map to two continuous adjacent patches in the Ca^{2+}-dependent EF2 binding sites in the S100A4 dimer (Fig. 5B) overlapping with the consensus ligand binding sites of S100 proteins [15]. Based on the localized changes in the NMR spectra, Ca^{2+}-dependence and mapping to the continuous regions, we concluded that the C-terminal region of CD5 specifically interacts with the EF2 sites of S100A4.

To test whether the interaction of S100A4 with CD5 could have any functional effect, CD5 was immunoprecipitated from resting E6.1 Jurkat cells and the kinase assays with the immune complexes were performed in the presence or absence of recombinant S100A4. The proteins that co-precipitated with CD5 had decreased phosphorylation in the presence of increasing concentrations of S100A4 (Supplementary Fig. S1). This suggests that S100A4 is able to disrupt CD5 complexes at the cell surface that could modify some of the receptor's effects, thus establishing S100A4 as a regulator of CD5 function.

4. Discussion

We show that metastasin S100A4 participates in the decision making for the proliferation and differentiation of antigen-exposed T-cells.

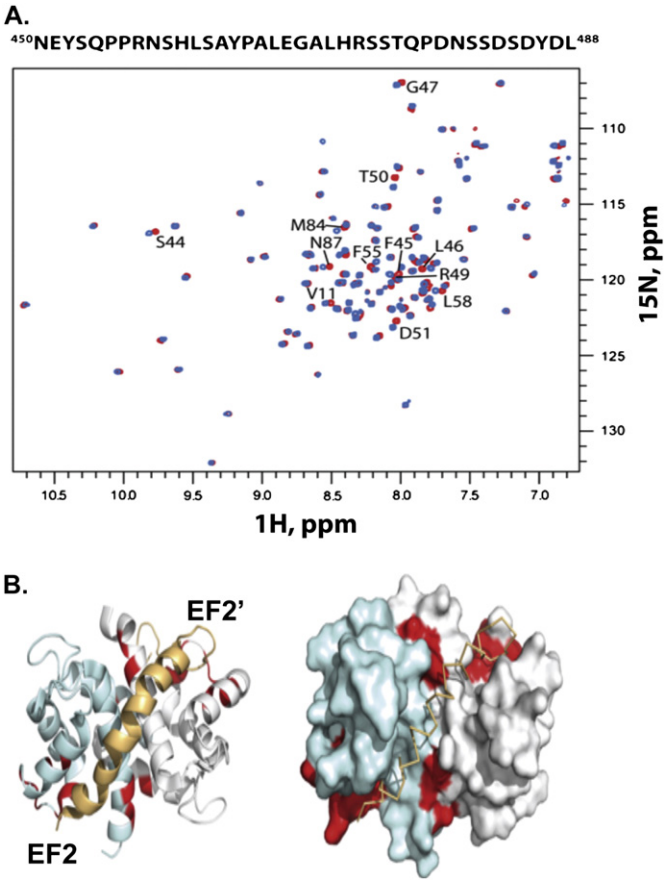

Fig. 5. Interaction between C100A4 and CD5 cytodomain was analysed by nuclear magnetic resonance spectrophotometry. A. Interaction of CD5 peptide with the Ca^{2+}-form of S100A4. Superposition of the ^{1}H,^{15}N-HSQC spectra (600 MHz) of 0.1 mM Ca^{2+}-S100A4 free in solution (red) and in the presence of 0.2 mM CD5 (aa 450–488) peptide (blue). Assignments of the cross-peaks corresponding to the significant chemical shift changes are marked in the spectrum of the free protein. B. Chemical shift changes induced by the CD5 peptide (aa 450–488) mapped on the structure of Ca^{2+}-S100A4 in complex with a myosin peptide (PDB ID: 2LNK) in cartoon (left) and surface (right) representation. Subunits of the S100A4 dimer are coloured in grey and light cyan, myosin peptide in orange. Residues corresponding to the significant chemical shift changes of (A) are highlighted in red. Ca^{2+}-dependent EF2 sites are marked.

S100A4KO mice showed an enhanced TCR-dependent proliferation capacity and increased IL2 production. This was combined with a reduced formation of effector T-cell populations and insufficient differentiation of Th17-cells recognized by the low synthesis of signature cytokine IL17A and low expression of the master transcription factor RORγt. Specificity of S100A4 inhibition for the acquisition of the described T-cell phenotype was demonstrated by the acute inhibition of the S100A4 gene transcription in WT mice by the specific shRNA-encoding construct, which yielded concordant results. The adoptive transfer of $CD4^+$ T cells from WT to S100A4KO mice resulted in a partially rescued phenotype of S100A4KO recipients and increased the population of $ROR\gamma t^+$ T-cells. The synthesis of the master transcription factor RORγt is critical for the formation of Th17 cells [46,47] and is controlled by a net of transcription factors consisting of Blimp-1–IRF4–STAT3 [41]. Both S100A4KO and S100A4-shRNA-treated mice had high levels of Blimp-1 and IRF4 mRNA, while the activity of STAT3 measured by pTyr705 was reduced.

Expression of STAT3 has recently emerged as an important molecular mechanism controlling the formation of Th17 cells [48] and their local accumulation in the inflamed RA synovia [49]. S100A4-deficient mice had the reduced synovial expression of pTyr705–STAT3 and reduced severity of arthritis. The spleen populations and the lymphocyte infiltrates in the synovial tissue of S100A4-deficient mice had a low number of $ROR\gamma t^+$ cells while the number of $Foxp3^+$ cells was increased. Th17 cells play an important role in the pathogenesis of RA mediating a link between the immune system and joints. Th17 cells produce high levels of the NF-γB dependent pro-inflammatory cytokines essential mediators of pathological processes in arthritis. Additionally Th17 cells are the cells supporting the formation of bone-resorbing osteoclasts and enhancing arthritic joint destruction [50,51]. We have recently reported impaired osteoclatogenesis with poor multinucleation, skewed expression of integrins and the low content of proteolytic enzymes in S100A4KO mice [37]. Thus, suppressing the formation of Th17 cells followed by the impaired osteoclastogenesis provides a plausible explanation to the alleviated joint damage observed in S100A4-deficient mice.

Herewith we asked which sequence of intracellular events could explain a connection between S100A4 and low STAT3 activity?

The activity of STAT3 is modulated through the pathway connecting integrins and the cytoskeletal remodelling protein RhoA [52,53] (see Graphical abstract). The activity of RhoA is promoted by the Src-kinase Fyn. The recruitment of Fyn to the inner leaflet of cellular membrane is coordinated by integrins [54–56]. We have previously shown that S100A4-deficient mice have impaired expression and stability of integrins on the surface of lymphocytes mobilised to the inflamed synovia [57] and on the bone marrow osteoclast progenitors [37]. Also, a potential interference of S100A4 in the RhoA system has been recently suggested to occur through its interaction with the scaffold protein rhotekin [17]. Thus, we searched for a potential functional coherence between S100A4 and Fyn and found that Fyn was shown to promote Th17 differentiation and functions as an upstream regulator of IRF4, RORγt, and IL17A [58].

The major function of Fyn in T-cells is the regulation of signalling through TCR where it works in synergy with the Src-tyrosine kinase Lck [59]. Lck and Fyn are known to control TCR signalling through the lymphocyte receptor CD5 (reviewed in [43,60]). The C-terminal phosphorylation of CD5 by Fyn has been recognized as a mechanism required for CD5-dependent regulation of Fyn [61]. Additionally, T-cell costimulation *via* the CD5 lymphocyte receptor has recently been shown to be critical for the activation of STAT3 and the initiation of Th17 development [48]. We observed, that the deficiency in S100A4 was associated with a smaller $CD5^+CD4^+$ T-cell population, which also had low levels of the phosphorylated pTyr453 CD5 expression on the surface of T-cells. A functional consequence of insufficient CD5 in S100A4-deficient mice may be found in the enhanced lymphocyte proliferative capacity observed both in S100A4KO and S100A4-shRNA-treated mice. Importantly, the transfer of $CD4^+$ T cells from WT mice enlarged the $CD5^+$ population and limited the lymphocyte proliferation of the S100A4KO recipients. Analogously to the S100A4-deficient mice, functional CD5 is shown to be essential for the differentiation of naïve T cells into Th2 and Th17-cells [42,48].

The interaction between S100A4 and its target proteins, NMMII, beta-liprin and recently the cytoplasmic domain of FcγRIIIA, occurs within the PKC or CK2 sensitive region of the target protein [13,14,16,23]. The cytoplasmic tail of CD5 contains the PKC-sensitive regions at Ser427 and the CK2 phosphorylation site at its C-terminal region [62]. A deletion of the C-terminal fragment of CD5 containing the CK2-phosphorylation site resulted in a failure to produce Th2 and Th17-cell subsets [63]. The binding assay revealed an interaction between S100A4 and a CD5 peptide containing the CK2-sensitive sequence resembling the affinity of smaller myosin peptides [64]. The results of the NMR spectra analysis provided an evidence for the physical interaction between the C-terminal-region of the CD5 cytoplasmic domain and the EF2 sites of S100A4. A dimerization of the CD5 receptor on the cell surface is expected to bring two S100A4 binding sites in each monomer close together and enhance the affinity between CD5 and S100A4.

In *in vitro* experiments we show that S100A4 co-precipitates with both Lck and Fyn from the cell lysates indicating a direct binding between these proteins. Moreover, this binding had a reciprocal effect on the kinase activity of Fyn and Lck. S100A4 reduced the Lck-dependent phosphorylation of CD5 to a degree comparable with the increase in the kinase activity of Fyn. This provides experimental evidence that S100A4 is able to disrupt CD5 complexes at the cell surface that could modify some of the receptor's effects, thus establishing S100A4 as a regulator of CD5 function. Thus, the absence of S100A4 corresponded to highest kinase activity of Lck, which is in agreement with the hyper-proliferation state observed in S100A4-deficient lymphocytes and predicted a disruption of Fyn activity. Insufficient formation of Th17 cells due to the reduced activity of STAT3 and the poor production of RoRγt is consistent with a Fyn-deficient phenotype [58]. These results suggest that S100A4 is essential for controlling a balance between the activities of Lck and Fyn tyrosine kinases. We hypothesised that S100A4 controls Lck-dependent T-cell proliferation and Fyn-dependent differentiation of T helper subsets through a CD5-dependent mechanism.

5. Conclusion

The present study demonstrates that the regulator of NMMII activity, metastasin S100A4 coordinates a balance between the proliferation and differentiation of antigen-exposed T-cells promoting CD5–Fyn–STAT3 dependent effects (Graphical abstract). S100A4-deficiency results in an impaired lineage differentiation of the Th17 subset of T helper cells. The reduced ability to form Th17 cells decreased the severity of arthritis in S100A4KO mice and reduced joint damage.

Supplementary data to this article can be found online at http://dx.doi.org/10.1016/j.bbadis.2014.07.003.

Disclosures

The authors have no financial conflicts of interests.

Acknowledgements

We thank Dr. Mariam Grigorian, Cancer Institute, Copenhagen, Denmark, for generously providing the breeding pairs of S100A4KO and WT mice.

This work has been funded by grants from the Swedish Research Council (MBo), the Medical Society of Göteborg (MBo), the Swedish Association against Rheumatism (MBo), the King Gustaf V:s 80-year Foundation (MBo), the Commission of European Union (FP7-Health 261460 to MBo and FP7-NMP4-LA-2009-228827 to ACM), the European Regional Development Fund through Programa Operacional

Factores de Competitividade (COMPETE), by the Portuguese Government through Fundação para a Ciência e a Tecnologia (PTDC/IMI-IMU/0158/2012 and PEst-C/SAU/LA0002/2011 to ACM), the Professor Nanna Swartz Foundation (MBo, MiB), the Torsten Söderberg's Foundation (MBo), the Rune and Ulla Amlövs Trust, the Ingabritt and Arne Lundberg's Foundation (MBo), the pharmacist Hedberg's Foundation (MiB), the Magnus Bergwall Foundation (MBo), the University of Gothenburg, the Family Thölen and Kristlers Foundation, and the Regional agreement on medical training and clinical research between the Western Götaland county council and the University of Göteborg (LUA/ALF, MBo). MBo holds the Medical Society of Gothenburg Chair in Rheumatology (Ingrid Högbergs Fond). Rita F. Santos holds a scholarship from the American Portuguese Biomedical Research Foundation. The funding sources have no involvement in study design; in the collection, analysis and interpretation of data; in the writing of the report; and in the decision to submit the article for publication.

References

[1] J.K. Eriksson, M. Neovius, S. Ernestam, S. Lindblad, J.F. Simard, J. Askling, Incidence of rheumatoid arthritis in Sweden: a nationwide population-based assessment of incidence, its determinants, and treatment penetration, Arthritis Care Res. 65 (2013) 870–878.
[2] N.C. Richman, J. Yazdany, J. Graf, V. Chernitskiy, J.B. Imboden, Extraarticular manifestations of rheumatoid arthritis in a multiethnic cohort of predominantly Hispanic and Asian patients, Medicine 92 (2013) 92–97.
[3] L.C. See, C.F. Kuo, I.J. Chou, M.J. Chiou, K.H. Yu, Sex- and age-specific incidence of autoimmune rheumatic diseases in the Chinese population: a Taiwan population-based study, Semin. Arthritis Rheum. 43 (2013) 381–386.
[4] C.M. Weyand, J.J. Goronzy, T-cell responses in rheumatoid arthritis: systemic abnormalities-local disease, Curr. Opin. Rheumatol. 11 (1999) 210–217.
[5] J.S. Smolen, D. Aletaha, M. Koeller, M.H. Weisman, P. Emery, New therapies for treatment of rheumatoid arthritis, Lancet 370 (2007) 1861–1874.
[6] P. Beemiller, M.F. Krummel, Mediation of T-cell activation by actin meshworks, Cold Spring Harb. Perspect. Biol. 2 (2010) a002444.
[7] M. Vicente-Manzanares, X. Ma, R.S. Adelstein, A.R. Horwitz, Non-muscle myosin II takes centre stage in cell adhesion and migration, Nat. Rev. Mol. Cell Biol. 10 (2009) 778–790.
[8] R.J. Salmond, A. Filby, I. Qureshi, S. Caserta, R. Zamoyska, T-cell receptor proximal signaling *via* the Src-family kinases, Lck and Fyn, influences T-cell activation, differentiation, and tolerance, Immunol. Rev. 228 (2009) 9–22.
[9] T. Ilani, G. Vasiliver-Shamis, S. Vardhana, A. Bretscher, M.L. Dustin, T cell antigen receptor signaling and immunological synapse stability require myosin IIA, Nat. Immunol. 10 (2009) 531–539.
[10] S. Kumari, S. Vardhana, M. Cammer, S. Curado, L. Santos, M.P. Sheetz, M.L. Dustin, T lymphocyte myosin IIA is required for maturation of the immunological synapse, Front. Immunol. 3 (2012) 230.
[11] K. Boye, G.M. Maelandsmo, S100A4 and metastasis: a small actor playing many roles, Am. J. Pathol. 176 (2010) 528–535.
[12] S.C. Garrett, K.M. Varney, D.J. Weber, A.R. Bresnick, S100A4, a mediator of metastasis, J. Biol. Chem. 281 (2006) 677–680.
[13] H.L. Ford, D.L. Silver, B. Kachar, J.R. Sellers, S.B. Zain, Effect of Mts1 on the structure and activity of nonmuscle myosin II, Biochemistry 36 (1997) 16321–16327.
[14] M. Kriajevska, M. Fischer-Larsen, E. Moertz, O. Vorm, E. Tulchinsky, M. Grigorian, N. Ambartsumian, E. Lukanidin, Liprin beta 1, a member of the family of LAR transmembrane tyrosine phosphatase-interacting proteins, is a new target for the metastasis-associated protein S100A4 (Mts1), J. Biol. Chem. 277 (2002) 5229–5235.
[15] P.R. Elliott, A.F. Irvine, H.S. Jung, K. Tozawa, M.W. Pastok, R. Picone, S.K. Badyal, J. Basran, P.S. Rudland, R. Barraclough, L.Y. Lian, C.R. Bagshaw, M. Kriajevska, I.L. Barsukov, Asymmetric mode of Ca^{2+}–S100A4 interaction with nonmuscle myosin IIA generates nanomolar affinity required for filament remodeling, Structure 20 (2012) 654–666.
[16] Z.H. Li, A. Spektor, O. Varlamova, A.R. Bresnick, Mts1 regulates the assembly of nonmuscle myosin-IIA, Biochemistry 42 (2003) 14258–14266.
[17] M. Chen, A.R. Bresnick, K.L. O'Connor, Coupling S100A4 to Rhotekin alters Rho signaling output in breast cancer cells, Oncogene 32 (2013) 3754–3764.
[18] J. van Dieck, M.R. Fernandez-Fernandez, D.B. Veprintsev, A.R. Fersht, Modulation of the oligomerization state of p53 by differential binding of proteins of the S100 family to p53 monomers and tetramers, J. Biol. Chem. 284 (2009) 13804–13811.
[19] G. Berge, D.E. Costea, M. Berg, H. Rasmussen, I. Grotterod, R.A. Lothe, G.M. Maelandsmo, K. Flatmark, Coexpression and nuclear colocalization of metastasis-promoting protein S100A4 and p53 without mutual regulation in colorectal carcinoma, Amino Acids 41 (2011) 875–884.
[20] G. Berge, G.M. Maelandsmo, Evaluation of potential interactions between the metastasis-associated protein S100A4 and the tumor suppressor protein p53, Amino Acids 41 (2011) 863–873.
[21] H. Chen, D.G. Fernig, P.S. Rudland, A. Sparks, M.C. Wilkinson, R. Barraclough, Binding to intracellular targets of the metastasis-inducing protein, S100A4 (p9Ka), Biochem. Biophys. Res. Commun. 286 (2001) 1212–1217.
[22] L.M. Orre, E. Panizza, V.O. Kaminskyy, E. Vernet, T. Graslund, B. Zhivotovsky, J. Lehtio, S100A4 interacts with p53 in the nucleus and promotes p53 degradation, Oncogene 32 (2013) 5531–5540.
[23] X. Li, J.G. Baskin, E.K. Mangan, K. Su, A.W. Gibson, C. Ji, J.C. Edberg, R.P. Kimberly, The unique cytoplasmic domain of human FcgammaRIIIA regulates receptor-mediated function, J. Immunol. 189 (2012) 4284–4294.
[24] R.R. Yammani, D. Long, R.F. Loeser, Interleukin-7 stimulates secretion of S100A4 by activating the JAK/STAT signaling pathway in human articular chondrocytes, Arthritis Rheum. 60 (2009) 792–800.
[25] O. Dmytriyeva, S. Pankratova, S. Owczarek, K. Sonn, V. Soroka, C.M. Ridley, A. Marsolais, M. Lopez-Hoyos, N. Ambartsumian, E. Lukanidin, E. Bock, V. Berezin, D. Kiryushko, The metastasis-promoting S100A4 protein confers neuroprotection in brain injury, Nat. Commun. 3 (2012) 1197.
[26] R.R. Yammani, C.S. Carlson, A.R. Bresnick, R.F. Loeser, Increase in production of matrix metalloproteinase 13 by human articular chondrocytes due to stimulation with S100A4: role of the receptor for advanced glycation end products, Arthritis Rheum. 54 (2006) 2901–2911.
[27] M.C. Erlandsson, L. Bian, I.M. Jonsson, K.M. Andersson, M.I. Bokarewa, Metastasin S100A4 is a mediator of sex hormone-dependent formation of the cortical bone, Mol. Endocrinol. 27 (2013) 1311–1321.
[28] I. Matsuura, K.N. Chiang, C.Y. Lai, D. He, G. Wang, R. Ramkumar, T. Uchida, A. Ryo, K. Lu, F. Liu, Pin1 promotes transforming growth factor-beta-induced migration and invasion, J. Biol. Chem. 285 (2010) 1754–1764.
[29] C.S. Boomershine, A. Chamberlain, P. Kendall, A.R. Afshar-Sharif, H. Huang, M.K. Washington, W.E. Lawson, J.W. Thomas, T.S. Blackwell, N.A. Bhowmick, Autoimmune pancreatitis results from loss of TGFbeta signalling in S100A4-positive dendritic cells, Gut 58 (2009) 1267–1274.
[30] J. Klingelhofer, L. Senolt, B. Baslund, G.H. Nielsen, I. Skibshoj, K. Pavelka, M. Neidhart, S. Gay, N. Ambartsumian, B.S. Hansen, J. Petersen, E. Lukanidin, M. Grigorian, Up-regulation of metastasis-promoting S100A4 (Mts-1) in rheumatoid arthritis: putative involvement in the pathogenesis of rheumatoid arthritis, Arthritis Rheum. 56 (2007) 779–789.
[31] L. Senolt, M. Grigorian, E. Lukanidin, B. Simmen, B.A. Michel, K. Pavelka, R.E. Gay, S. Gay, M. Neidhart, S100A4 is expressed at site of invasion in rheumatoid arthritis synovium and modulates production of matrix metalloproteinases, Ann. Rheum. Dis. 65 (2006) 1645–1648.
[32] M.C. Erlandsson, K. Forslind, S.E. Andersson, A. Lund, M.I. Bokarewa, Metastasin S100A4 is increased in proportion to radiographic damage in patients with RA, Rheumatology 51 (2012) 932–940.
[33] L. Oslejskova, M. Grigorian, H. Hulejova, J. Vencovsky, K. Pavelka, J. Klingelhofer, S. Gay, M. Neidhart, H. Brabcova, D. Suchy, L. Senolt, Metastasis-inducing S100A4 protein is associated with the disease activity of rheumatoid arthritis, Rheumatology 48 (2009) 1590–1594.
[34] C. El Naaman, B. Grum-Schwensen, A. Mansouri, M. Grigorian, E. Santoni-Rugiu, T. Hansen, M. Kriajevska, B.W. Schafer, C.W. Heizmann, E. Lukanidin, N. Ambartsumian, Cancer predisposition in mice deficient for the metastasis-associated Mts1(S100A4) gene, Oncogene 23 (2004) 3670–3680.
[35] B. Grum-Schwensen, J. Klingelhofer, C.H. Berg, C. El-Naaman, M. Grigorian, E. Lukanidin, N. Ambartsumian, Suppression of tumor development and metastasis formation in mice lacking the S100A4(mts1) gene, Cancer Res. 65 (2005) 3772–3780.
[36] M. Dehlin, S. Andersson, M. Erlandsson, M. Brisslert, M. Bokarewa, Inhibition of fms-like tyrosine kinase 3 alleviates experimental arthritis by reducing formation of dendritic cells and antigen presentation, J. Leukoc. Biol. 90 (2011) 811–817.
[37] M.C. Erlandsson, M.D. Svensson, I.M. Jonsson, L. Bian, N. Ambartsumian, S. Andersson, Z. Peng, J. Vaaraniemi, C. Ohlsson, K.M. Andersson, M.I. Bokarewa, Expression of metastasin S100A4 is essential for bone resorption and regulates osteoclast function, Biochim. Biophys. Acta 1833 (2013) 2653–2663.
[38] S.S. Lindblad, P. Mydel, A. Hellvard, I.M. Jonsson, M.I. Bokarewa, The N-methyl-D-aspartic acid receptor antagonist memantine ameliorates and delays the development of arthritis by enhancing regulatory T cells, Neurosignals 20 (2012) 61–71.
[39] M.A. Castro, R.J. Nunes, M.I. Oliveira, P.A. Tavares, C. Simoes, J.R. Parnes, A. Moreira, A.M. Carmo, OX52 is the rat homologue of CD6: evidence for an effector function in the regulation of CD5 phosphorylation, J. Leukoc. Biol. 73 (2003) 183–190.
[40] W.F. Vranken, W. Boucher, T.J. Stevens, R.H. Fogh, A. Pajon, M. Llinas, E.L. Ulrich, J.L. Markley, J. Ionides, E.D. Laue, The CCPN data model for NMR spectroscopy: development of a software pipeline, Proteins 59 (2005) 687–696.
[41] N. Yosef, A.K. Shalek, J.T. Gaublomme, H. Jin, Y. Lee, A. Awasthi, C. Wu, K. Karwacz, S. Xiao, M. Jorgolli, D. Gennert, R. Satija, A. Shakya, D.Y. Lu, J.J. Trombetta, M.R. Pillai, P.J. Ratcliffe, M.L. Coleman, M. Bix, D. Tantin, H. Park, V.K. Kuchroo, A. Regev, Dynamic regulatory network controlling TH17 cell differentiation, Nature 496 (2013) 461–468.
[42] R.C. Axtell, L. Xu, S.R. Barnum, C. Raman, CD5–CK2 binding/activation-deficient mice are resistant to experimental autoimmune encephalomyelitis: protection is associated with diminished populations of IL-17-expressing T cells in the central nervous system, J. Immunol. 177 (2006) 8542–8549.
[43] G. Soldevila, C. Raman, F. Lozano, The immunomodulatory properties of the CD5 lymphocyte receptor in health and disease, Curr. Opin. Immunol. 23 (2011) 310–318.
[44] H.M. Oh, C.R. Yu, N. Golestaneh, A. Amadi-Obi, Y.S. Lee, A. Eseonu, R.M. Mahdi, C.E. Egwuagu, STAT3 protein promotes T-cell survival and inhibits interleukin-2 production through up-regulation of Class O Forkhead transcription factors, J. Biol. Chem. 286 (2011) 30888–30897.
[45] K.E. Burgess, M. Yamamoto, K.V. Prasad, C.E. Rudd, CD5 acts as a tyrosine kinase substrate within a receptor complex comprising T-cell receptor zeta chain/CD3 and protein-tyrosine kinases p56lck and p59fyn, Proc. Natl. Acad. Sci. U. S. A. 89 (1992) 9311–9315.

[46] I.I. Ivanov, B.S. McKenzie, L. Zhou, C.E. Tadokoro, A. Lepelley, J.J. Lafaille, D.J. Cua, D.R. Littman, The orphan nuclear receptor RORγt directs the differentiation program of proinflammatory IL-17^{+} T helper cells, Cell 126 (2006) 1121–1133.
[47] N. Manel, D. Unutmaz, D.R. Littman, The differentiation of human T(H)-17 cells requires transforming growth factor-beta and induction of the nuclear receptor RORgammat, Nat. Immunol. 9 (2008) 641–649.
[48] J. de Wit, Y. Souwer, A.J. van Beelen, R. de Groot, F.J. Muller, H. Klaasse Bos, T. Jorritsma, M.L. Kapsenberg, E.C. de Jong, S.M. van Ham, CD5 costimulation induces stable Th17 development by promoting IL-23R expression and sustained STAT3 activation, Blood 118 (2011) 6107–6114.
[49] J.H. Ju, Y.J. Heo, M.L. Cho, J.Y. Jhun, J.S. Park, S.Y. Lee, H.J. Oh, S.J. Moon, S.K. Kwok, K.S. Park, S.H. Park, H.Y. Kim, Modulation of STAT-3 in rheumatoid synovial T cells suppresses Th17 differentiation and increases the proportion of Treg cells, Arthritis Rheum. 64 (2012) 3543–3552.
[50] J. Kikuta, Y. Wada, T. Kowada, Z. Wang, G.H. Sun-Wada, I. Nishiyama, S. Mizukami, N. Maiya, H. Yasuda, A. Kumanogoh, K. Kikuchi, R.N. Germain, M. Ishii, Dynamic visualization of RANKL and Th17-mediated osteoclast function, J. Clin. Invest. 123 (2013) 866–873.
[51] K. Sato, A. Suematsu, K. Okamoto, A. Yamaguchi, Y. Morishita, Y. Kadono, S. Tanaka, T. Kodama, S. Akira, Y. Iwakura, D.J. Cua, H. Takayanagi, Th17 functions as an osteoclastogenic helper T cell subset that links T cell activation and bone destruction, J. Exp. Med. 203 (2006) 2673–2682.
[52] D. Kesanakurti, C. Chetty, D. Rajasekhar Maddirela, M. Gujrati, J.S. Rao, Essential role of cooperative NF-kappaB and Stat3 recruitment to ICAM-1 intronic consensus elements in the regulation of radiation-induced invasion and migration in glioma, Oncogene 32 (2013) 5144–5155.
[53] K.H. Shain, D.N. Yarde, M.B. Meads, M. Huang, R. Jove, L.A. Hazlehurst, W.S. Dalton, Beta1 integrin adhesion enhances IL-6-mediated STAT3 signaling in myeloma cells: implications for microenvironment influence on tumor survival and proliferation, Cancer Res. 69 (2009) 1009–1015.
[54] X. Liang, N.A. Draghi, M.D. Resh, Signaling from integrins to Fyn to Rho family GTPases regulates morphologic differentiation of oligodendrocytes, J. Neurosci. 24 (2004) 7140–7149.
[55] L.A. Samayawardhena, R. Kapur, A.W. Craig, Involvement of Fyn kinase in Kit and integrin-mediated Rac activation, cytoskeletal reorganization, and chemotaxis of mast cells, Blood 109 (2007) 3679–3686.
[56] K.K. Wary, A. Mariotti, C. Zurzolo, F.G. Giancotti, A requirement for caveolin-1 and associated kinase Fyn in integrin signaling and anchorage-dependent cell growth, Cell 94 (1998) 625–634.
[57] L. Bian, P. Strzyz, I.M. Jonsson, M. Erlandsson, A. Hellvard, M. Brisslert, C. Ohlsson, N. Ambartsumian, M. Grigorian, M. Bokarewa, S100A4 deficiency is associated with efficient bacterial clearance and protects against joint destruction during Staphylococcal infection, J. Infect. Dis. 204 (2011) 722–730.
[58] A. Ueda, L. Zhou, P.L. Stein, Fyn promotes Th17 differentiation by regulating the kinetics of RORgammat and Foxp3 expression, J. Immunol. 188 (2012) 5247–5256.
[59] A. Filby, B. Seddon, J. Kleczkowska, R. Salmond, P. Tomlinson, M. Smida, J.A. Lindquist, B. Schraven, R. Zamoyska, Fyn regulates the duration of TCR engagement needed for commitment to effector function, J. Immunol. 179 (2007) 4635–4644.
[60] D. Filipp, O. Ballek, J. Manning, Lck, membrane microdomains, and TCR triggering machinery: defining the new rules of engagement, Front. Immunol. 3 (2012) 155.
[61] M. Bamberger, A.M. Santos, C.M. Goncalves, M.I. Oliveira, J.R. James, A. Moreira, F. Lozano, S.J. Davis, A.M. Carmo, A new pathway of CD5 glycoprotein-mediated T cell inhibition dependent on inhibitory phosphorylation of Fyn kinase, J. Biol. Chem. 286 (2011) 30324–30336.
[62] C. Raman, R.P. Kimberly, Differential CD5-dependent regulation of CD5-associated CK2 activity in mature and immature T cells: implication on TCR/CD3-mediated activation, J. Immunol. 161 (1998) 5817–5820.
[63] C.M. Sestero, D.J. McGuire, P. De Sarno, E.C. Brantley, G. Soldevila, R.C. Axtell, C. Raman, CD5-dependent CK2 activation pathway regulates threshold for T cell anergy, J. Immunol. 189 (2012) 2918–2930.
[64] S.K. Badyal, J. Basran, N. Bhanji, J.H. Kim, A.P. Chavda, H.S. Jung, R. Craig, P.R. Elliott, A. F. Irvine, I.L. Barsukov, M. Kriajevska, C.R. Bagshaw, Mechanism of the Ca^{2+}-dependent interaction between S100A4 and tail fragments of nonmuscle myosin heavy chain IIA, J. Mol. Biol. 405 (2011) 1004–1026.